equilibrium using d' Alembert's principle. In modeling of drillstring it is simpler to consider energy principal as energy is a scalar quantity, independent on the choice of coordinate system and can easily deal with multi-degrees of freedom systems with the help of the generalized coordinates which describe the system. This, in this work, the Lagrange's equation is used to derive the system's equations of motion.

$$L = T - U \tag{1}$$

$$\frac{d}{dt}\left(\frac{\delta L}{\delta \dot{q}_i}\right) - \frac{\delta L}{\delta q_i} + \frac{\delta D}{\delta \dot{q}_i} = F_i \tag{2}$$

where:
q_i: generalized coordinate (Degree of Freedom).
D: Rayleigh dissipation function.
F_i: generalized force along a particular generalized coordinate.

2.2 Kinetic and Potential Energies

The Kinetic energy of the system can be written as:

$$T_{total} = T_M + T_b \tag{3}$$

where:
T_M: Kinetic energy of the rotor.
T_b: Kinetic energy of the unbalance mass. Hence

$$T_M = \frac{1}{2}M(\dot{x}^2 + \dot{y}^2) + \frac{1}{2}I_o(\dot{\theta} + \dot{\gamma})^2 \tag{4}$$

and,

$$T_b = \frac{1}{2}m_b {v_b}^2 \tag{5}$$

where:
v_b: unbalanced mass velocity.

the position of the unbalance mass at an instant can be written as:

$$\overrightarrow{x_b} = [x + e\cos(\theta + \gamma)]i + [y + e\sin(\theta + \gamma)]j \tag{6}$$

Then the T_{total} can be written as:

$$\begin{aligned} T_{total} = \frac{1}{2}M(\dot{x}^2 + \dot{y}^2) + \frac{1}{2}I_o(\dot{\theta} + \dot{\gamma})^2 \\ + \left(\frac{1}{2}m_b\right)\left[\{\dot{x} - e(\dot{\theta} + \dot{\gamma})\sin(\theta + \gamma)\}^2\right. \\ \left. + \{(\dot{y} + e(\dot{\theta} + \dot{\gamma})\cos(\theta + \gamma)\}^2\right] \end{aligned} \tag{7}$$

The system's total potential energy can be divided into three terms, namely, U_x, U_y and U_{tor}. Where U_x, U_y and U_{tor} are the potential energies along the *x, y* and torsional direction, respectively. Therefore, the total potential energy can be written as follows:

$$U_{total} = U_x + U_y + U_{tor} \tag{8}$$

Utilizing the Lagrange formulation in three degrees of freedom given in Eq. 5 and the set of equations for kinetic and potential energies, yield the following three equations of motion for the system:

$$(M + m_b)\ddot{x} + c_b\dot{x} + k_b x = m_b e\left[(\ddot{\theta} + \ddot{\gamma})\sin(\theta + \gamma) + (\dot{\theta} + \dot{\gamma})^2\cos(\theta + \gamma)\right] \tag{9}$$

$$(M + m_b)\ddot{y} + c_b y + k_b y = m_b e\left[(\dot{\theta} + \dot{\gamma})^2\sin(\theta + \gamma) - (\ddot{\theta} + \ddot{\gamma})\cos(\theta + \gamma)\right] \tag{10}$$

$$I\ddot{\gamma} + c_{tor}\dot{\gamma} + k_{tor}\gamma = m_b e[(\ddot{x}\sin(\theta + \gamma)) - (\ddot{y}\cos(\theta + \gamma))] + T_{tor} \tag{11}$$

where, $I = I_o + m_b e^2$

Eqs. (9-11) are nonlinear ordinary differential equations. These set of equations were solved numerically using fourth-order Runge–Kutta Algorithm in Matlab software. The outcome of applying this Algorithm is presented in the results and discussion section.

3 Experimental Approach

A novel in-house experimental setup capable of imitating downhole lateral and torsional vibrations has been designed and constructed. In this work, vibration coupling effects and interactions between various phenomena such as whirling, and parametric excitation are investigated. Parameters of experimental setup have been adopted to validate the previously developed mathematical model. This helps reducing drillstring failures as well as provides satisfactory answers and justifications about uncertainty and performance of the drillstring under various loading and operating conditions. Fig. 3 (a, b) shows the experimental setup and schematic of the setup and its individual components. Table 1 lists representations for the numbers of components. Fig. 4 (a, b) shows torque measurement system fixed to the drillstring and the induced lateral vibration is represented by an eccentric mass. To induce torsional vibration, a braking mechanism is adopted. In this work, the breaking mechanism is constrained to brake at fixed duration and steady applied torque while allowing multiple numbers of brakes.

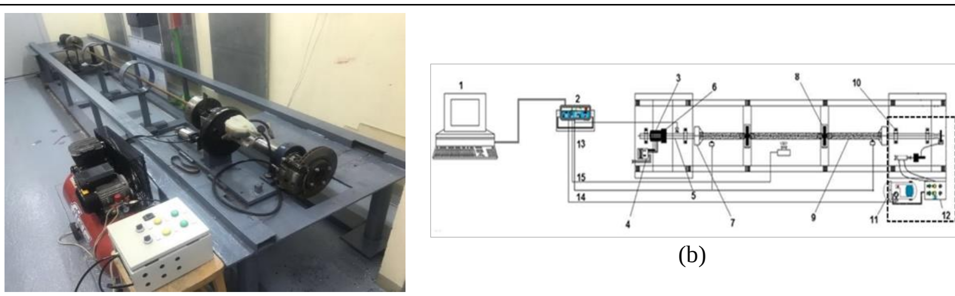

(a) (b)

Fig. 3. Experimental Setup (a) and its individual components schematics (b)

Table 1: Main components of the experimental setup

Components/ Systems	Part name
1	Computer
2	Data acquisition system
3	3-plase electrical motor
4	Speed controller
5	Shaft
6	Sprocket and Chain
7	Chuck and flange assembly
8	Stabilizer
9	Specimen (Tube)
10	Ball bearing
11	Compressor
12	Brake system controller
13	Hall effect sensor
14	Brake on/off switch
15	Ultrasonic sensor
16	Torque Measurement System

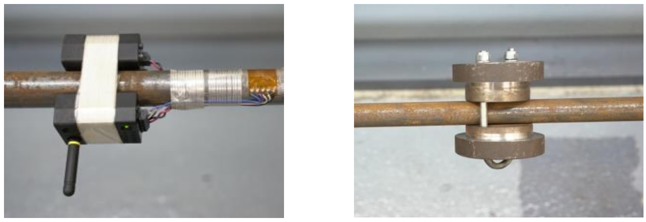

(a) (b)

Fig. 4. Torque measurement system (a) and Unbalanced mass

4 Results and Discussions

4.1 Parameters and Results of the Mathematical Approach

4.1.1 Undamped rotor rotating at critical speed:

The undamped system is examined and shown that the critical speed occurs when $\dot{\theta} = w_{n,b}$. and $c_b = 0$. Fig. 5 (a) shows that lateral deflections are continuously increased as undamped system is operated at its critical speed. Hence, rotating close to its critical speed maximum values of deflections are reached. Fig. 5 (b) shows trajectories of horizontal and vertical deflections of undamped shaft rotating at critical speed.

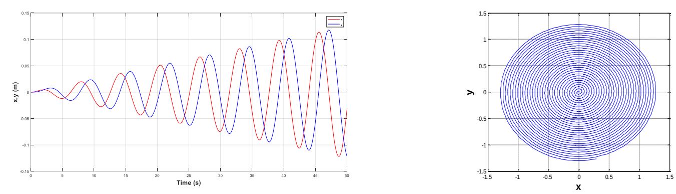

(a) (b)

Fig. 5. Undamped system lateral deflections (a) and trajectories horizontal and vertical deflections of undamped shaft (b).

4.1.2 Effect of Bending damping ratio on rotor's response

The effect of bending damping ratio on the rotor's response was investigated by changing the value of the damping coefficient. The effects of changing damping ratio ($\zeta_b = 0.05, 0.07 \,\&\, 0.1$) on transient response and magnitude of deflection were observed. It is lengthy to reproduce complete results here. A representative trend is depicted in Fig. 6 (a, b). Increasing the bending ratio, the time required to reach steady state response and deflections are reduced. This is due to the increase in the dissipated energy of the system.

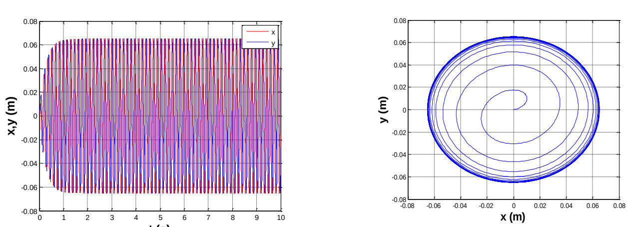

(a) (b)

Fig. 6. Effects of changing damping ratio at $\zeta_b = 0.1$ on deflections (a) and trajectories (b).

Three other important effects include (*i*) the effect of unbalanced mass on the rotor's response, (*ii*) the effect of bending damping ratio on the rotor's response due to change in damping coefficients and (*iii*) the effect of reverse torque on the rotor's response were all thoroughly investigated. The reader may refer to the authors study [16].

4.2 Experimental results

The experiments were carried out under controlled conditions to examine the setup performance, and to investigate the effects of induced lateral vibration on the drill string fatigue failure. Sets of drill strings of 1", 2" and 3" outer diameter and 5m long were used. Initial tests were performed by rotating the drillstring on various rotational speed and lateral amplitudes were observed. Fig. 7 shows the rotational speed vs. lateral deflections for the three drillstrings. It shows that the amplitudes are lower in larger drillstring diameters at same rotational speed. In addition, the lateral amplitude is higher for higher speed for the same drillstring dimensions.

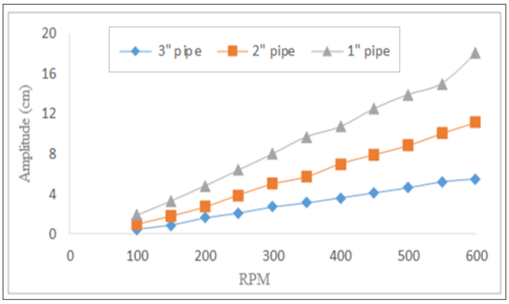

Fig. 7. Drillstrings behavior at various rotational speeds

Fig. 8 illustrates that the maximum lateral amplitude occurs in the middle of the drillstring. Lateral vibration in a drillstring often results from eccentricity which leads to centripetal forces at particular rotational speeds. When external excitations (rotating the drillstring) take place close to lateral natural frequencies, the amplitude of lateral vibration remarkably increases and hence the drillstring strikes wellbore wall and creates considerable shocks.

Fig. 8. Large lateral amplitude for 1" drillstring near its rotational critical speed.

Conclusions

This work aimed at gaining a deeper understanding of the complex behavior of drillstring under vibrations and its detrimental effect on drilling operation. The developed model imitates real drillstring behavior inside the wellbore with regards to its dynamic movements based on modeling an in-house constructed testing rig which mimic the real drilling field operations. The Lagrangian approach is used to obtain the drillstring lateral and torsional vibration coupling equations of motion. A mathematical model is developed to simulate the dynamic behavior of the drillstring. The effects of lateral and torsional vibrations and whirling motion of the drillstring are included in the model. An experimental setup was developed to imitate the vibration modes induced in the drillstring when it runs downhole in oil or gas wells. The testing facility is capable of investigating effects of individual and coupled modes on vibration on drill string failure. Results showed that the lateral amplitude versus number of stress cycles behavior is similar to the familiar fatigue S-N curve. Torsional vibration is induced in the drillstring by applying a constant reversed torque utilizing the braking mechanism in the drillstring at multiple numbers of brakes. Results showed that multiple numbers of braking, which represent frequent stick-slip, leads to fatigue failure unless the system's critical operating speeds and design parameters are determined and implemented for a safe drilling. The developed model predicted that the vibrations induced in the drillstring due to the interaction with the wellbore are the main reason for drillstring failure. Established models provides a basis for understanding fatigue failure and leads to prediction of safe operation and long service life of drillstrings.

References

1. Macdonald, K.A., Bjune, J.V., 2007, "Failure analysis of drillstrings," Engineering Failure Analysis, 14, pp. 1641-1666.
2. Moradi, S., Ranjbar, K., 2009, "Experimental and computational failure analysis of drillstrings. Engineering Failure Analysis," 16, pp. 923-933.
3. Reid, D., Rabja, H., 1995, "Analysis of drill string failure," Presented in 1995 SPE drilling conference, Amsterdam.
4. Jardine, S., Malone, D., Sheppard, M., 1994, "Putting a damper on drilling's bad vibrations," Oilfield Review, 1, pp. 15-20.
5. Spanos, P.D., Chevallier, A.M., Politis, N.P., Payne, M.L., 2003, "Oil well drilling: a vibrations perspective," The Shock and Vibration Digest, 35(2), pp. 81-99.
6. Khulief, Y.A., Al-Naser, H., 2005, "Finite element dynamic analysis of drill strings," Finite Element Analysis and Design, 41, pp. 1270-1288.
7. Berlioz, A., Der Hagopian, J., Dufour, R, Draoui, E., 1996, "Dynamic behaviour of drill-string: experimental investigation of lateral instabilities," Transaction of the American Society of Mechanical Engineers, Journal of Vibration and Acoustics, 118(3), pp. 292-298.
8. Yigit, A.S., Christofourou, A.P., 1996, "Coupled axial and transverse vibrations of oil well drillstrings," Journal of Sound and Vibration, 195(4), pp. 617-627.
9. Baryshnikoy, A., Calderoni, A., Ligrone, A., Ferrara, P., 1997, "A new to the analysis of drillstring fatigue behaviour," SPE Drilling and Completion, 12(2), pp. 77-84.
10. Abdo, J., 2011, "Analytical approach to estimate amplitude of stick-slip oscillations," Journal of Theoretical and Applied Mechanics, 49(4), pp 971-986.
11. Farhang, K., Lim, A., 2007, "A kinetic friction model for viscoelastic contact of nominally flat rough surfaces," Journal of Tribology, 129 (3), pp. 684-688.
12. Yigit, A.S., Christoforou, A.P., 1998. Coupled torsional and bending vibrations of drillstrings subject to impact with friction. Journal of Sound and Vibration. 215(1), 167–181.
13. Ghasemloonia, A., Rideout, D.G., Butt, S.D., 2015. A review of drillstring vibration modeling and suppression methods. Journal of Petroleum Science and Engineering. 131(1), 150-164.
14. Abdo, J., 2006, "Modelling of Frictional Contact Parameters of a Mechanical Systems," International Journal of Applied Mechanics and Engineering, 11(3), pp 449-465.
15. J. Abdo, E. Hassan, A. Al-Shabibi and J. Kwak (2017) "Design of a Testing Facility for Investigation of Drill Pipes Fatigue Failure" The Journal of Engineering Research V. 14 (2), p 1-7.
16. J. Abdo, E. Hassan, K. Boulbrachene and J. Kwak (2018), "Drillstring Failure-Identification, Modeling and Experimental Characterization", ASCE-ASME J. of Risk and Uncertainty in Eng. Systems